Catalyst-Assisted Vapor−Liquid−Solid Growth of Single-Crystal CdS Nanobelts and Their Luminescence Properties

Tao Gao* and Taihong Wang

Institute of Physics, Chinese Academy of Sciences, P.O. Box 603, Beijing 100080, People's Republic of China

Received: June 9, 2004; In Final Form: October 11, 2004

Mass production of CdS nanobelts is successfully achieved by a simple thermal evaporation of CdS powders under controlled conditions in the presence of Au catalysts. The as-synthesized CdS nanobelts are single-crystalline with wurtzite structure, usually several hundred nanometers in width, tens of micrometers in length, and tens of nanometers in thickness. The room-temperature photoluminescence spectrum of CdS nanobelts features three luminescence peaks around 504, 513, and 770 nm, which are attributed to the band-edge, band-to-band and surface state emissions, respectively. The growth of CdS nanobelts is initiated by Au catalyst nanoparticles via a catalyst-assisted vapor−liquid−solid process, and a side growth along the belt width direction via a vapor−solid process is also suggested. This synthetic method offers the possibility for the control of CdS nanobelts on a special substrate, which would be of particular interest for their applications in optoelectronic devices.

1. Introduction

Semiconductor nanobelts (NBs), having a rectangular cross section with a well-defined geometry and perfect crystallinity, have been reported as a new subgroup of one-dimensional (1D) nanostructures[1] that are distinctly different from the hollow nanotubes (NTs)[2] and solid nanowires (NWs).[3] Semiconductor NBs possess interesting and useful physical properties and can be used as appealing nanoscale building blocks to assemble functional nanodevices such as chemical sensors,[4,5] cantilevers,[6] and field effect transistors.[7] In this regard, critical to the properties and behaviors of these and other potential nanodevices are the sizes, crystallinity, and stoichiometry of the semiconductor NBs.[8] Thus, the development of efficient synthetic methods that enable mass production and precise control of semiconductor NBs is expected to have a significant impact on progress.

Over the past few years, a variety of synthetic methods have been developed to produce a number of interesting NB systems such as ZnO,[1,10−12] SnO_2,[7,13−15] Ga_2O_3,[16,17] MgO,[18,19] ZnS,[20−24] and CdS.[25−27] Among them, CdS is an important II−IV semiconductor and deserves particular attention owing to its suitable band gap energy and wide optoelectronic applications such as in lasers, light-emitting diodes, and luminescence devices.[28−31] Recently, synthesis of CdS NBs has attracted great interest.[25−27] For example, Dong et al. have prepared CdS NBs and NWs on a tungsten substrate.[25] Li and co-workers have prepared CdS NBs by using a vapor−solid (VS) growth method.[26] Zhang et al. have also reported the preparation of CdS NBs by vapor transport.[27] It should be pointed out that, as the most conventional method for the synthesis of semiconductor NBs, the VS growth process has demonstrated considerable flexibility in fabricating a wide range of NB systems.[1,10−20] However, the difficulty in controlling nucleation in the VS growth has limited the size control of the products.[8] Recent progress[24,25,32] has shown that the semiconductor NBs can be produced via a catalyst-assisted vapor−liquid−solid (VLS) growth mechanism. The VLS growth mechanism has been known for a long time[33] and has been used widely in fabricating a range of semiconductor NW systems.[8,25,34] For growth of NWs by the VLS process, the key is to generate nanosized catalyst clusters that define their size and direct the 1D growth.[35] Studies reveal that the nucleation sites[36] and diameters[35] of semiconductor NWs can be easily controlled during the VLS process.[3,8,9] However, up to now, details on the formation of NBs with a rectangular cross section and high width-to-thickness ratio via the VLS growth process have not been very clear.[24,25,32]

In this study, mass production of single-crystal CdS NBs with controllable morphology and size has been successfully achieved by a simple thermal evaporation of CdS powders under controlled conditions in the presence of Au catalysts. The factors that affect the size and the morphology of CdS NBs are discussed in this paper. It is found that the growth of CdS nanobelts is initiated by Au catalyst nanoparticles via the catalyst-assisted VLS growth process, and simultaneously, a side growth along the belt width direction via the VS growth process is observed. This synthetic method offers the possibility for the control of CdS NBs on a special substrate, which would be of particular interest for their applications in optoelectronic devices. Moreover, luminescence properties of the as-synthesized CdS NBs are also investigated.

2. Experimental Procedures

Our fabrication method is based on thermal evaporation of CdS powders under controlled conditions in the presence of Au catalysts. A quartz tube was mounted horizontally inside a high-temperature tube furnace. An alumina crucible filled with 2 g of CdS powders (AR grade) was placed in the middle of the quartz tube at the center of the furnace. Si substrates were first coated with a layer of a Au thin film (about 10 nm) and then placed downstream in the tube. Prior to heating, the system was flushed with high-purity Ar for 30 min to eliminate O_2. Ar was introduced into the quartz tube through a mass-flow controller at a rate of 120 standard cubic centimeters per minute (sccm). The temperature of the furnace was rapidly increased

* To whom correspondence should be addressed. Phone: +86-10-82649540. Fax: +86-10-82649531. E-mail: tgaoztian@163.net.

10.1021/jp047519s CCC: $27.50
Published on Web 11/24/2004

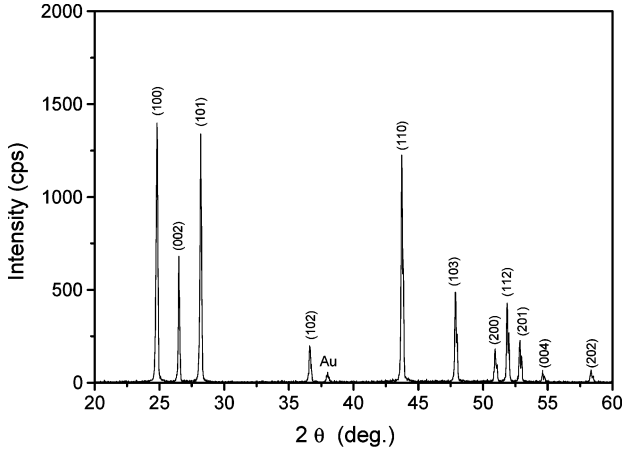

Figure 1. XRD pattern of the as-synthesized CdS NBs.

to 840 °C from room temperature within 2 min and held at this temperature for different times from 30 min to 4 h under the constant Ar flow. The growth temperature of the CdS NBs on Au-coated Si substrates was controlled by adjusting the distance between the crucible and the Si substrates. After the furnace was cooled naturally to room temperature, the Ar flow was turned off. It was observed that yellow wool-like products in high yield were formed on the surface of the Si substrates. Structures of the as-synthesized CdS NBs were characterized by using powder X-ray diffraction (XRD; D/Max-2400 with Cu Kα radiation), field-emission scanning electron microscopy (FE-SEM; XL30 S-FEG), transmission electron microscopy (TEM; JEM-2010), energy-dispersive X-ray spectroscopy (EDS), and selected area electron diffraction (SAED). Photoluminescence (PL) measurements were carried out on an RPM 2000 UV−vis spectrophotometer using a He−Cd laser line of 325 nm as an excitation source. All the characterizations were performed at room temperature.

3. Results and Discussion

3.1 Structural Characteristics of CdS NBs. Figure 1 shows a typical XRD pattern of the as-synthesized products. The diffraction peaks can be perfectly indexed to the wurtzite CdS. The CdS lattice constants obtained by refinement of XRD data for the as-prepared CdS are $a = 0.413$ nm and $c = 0.671$ nm within experimental error, and are consistent with those of bulk wurtzite CdS (JCPDS 41-1049), revealing that the as-synthesized products are crystalline CdS with wurtzite structure. Also, a weak Au diffraction peak was observed, which results from the Au catalyst particles.

Figure 2a shows a representative FE-SEM image of the as-prepared CdS deposited on the Au-coated Si substrates. The products consist of a large quantity of 1D nanostructures with a typical width of about several hundred nanometers and length of about tens to several hundred micrometers. A high-magnification FE-SEM image (Figure 2b) of several curved CdS 1D nanostructures reveals that their geometrical shape is beltlike and their thickness is about 30−60 nm.

It is also found that, at the ends of these CdS NBs, as shown in Figure 3a, the width gradually decreases along the growth direction and terminates at a particle located at the belt tip. A higher magnification image in the upper-left inset shows that a particle-like material caps the end of the belt. EDS measurements made on the belt stem (Figure 3b) and the particle-like material (Figure 3c) indicate that the belt stem is only composed of Cd and S, while the particle is composed of Au, S, and Cd. EDS analysis of the NBs demonstrates that a 1:1 Cd/S composition within experimental error is consistent with stoichiometric CdS. The existence of Au−CdS alloy particles capped at the end of the produced NBs suggests that a Au-catalyzed VLS process[8,34] is involved for the growth of CdS NBs.

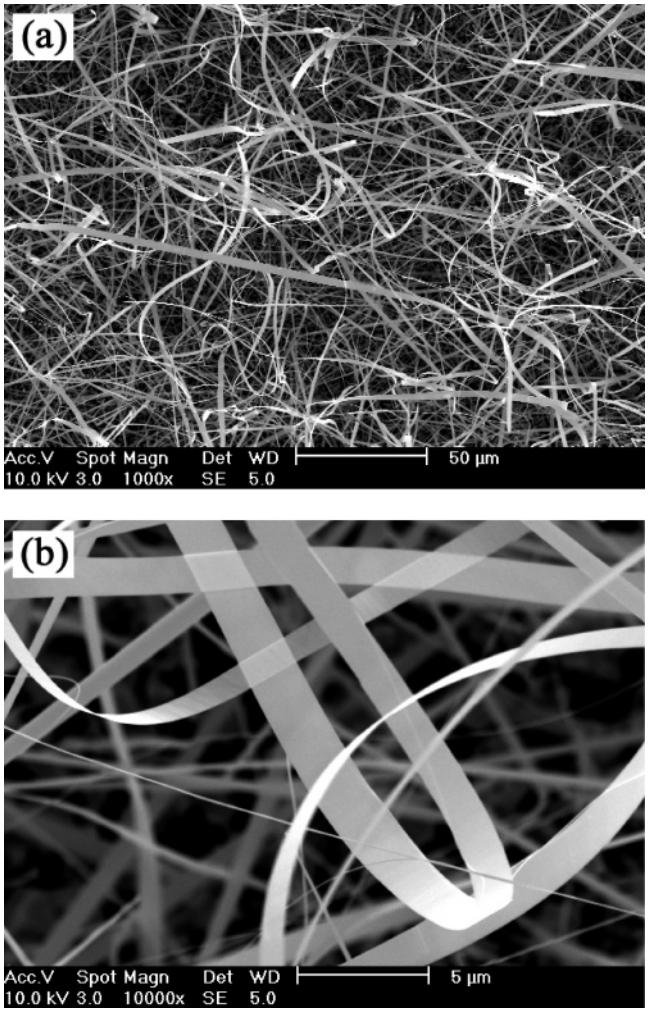

Figure 2. (a) Low- and (b) high-magnification FE-SEM images of the CdS NBs deposited on the Si substrates. The growth time and temperature are 1 h and 650 °C, respectively.

Detailed microstructure information of the CdS NBs is further characterized by TEM. A representative TEM image shown in Figure 4a reveals that the produced CdS NBs are relatively uniform with a typical width and thickness of about 200 and 40 nm, respectively. The CdS NBs are almost electron transparent, which further suggests that the thickness of the NBs is small. The ripple-like line in the TEM image is due to the bending of the belts.[1] The inset of Figure 4a shows a corresponding SAED pattern recorded with an electron beam perpendicular to the long axis of the belt. The SAED patterns are essentially identified over the entire belt, indicating the single-crystalline nature of the CdS NBs. Moreover, the SAED pattern can be indexed for the [010] zone axis of single-crystalline CdS, indicating that the belt growth occurs along the ⟨101⟩ direction. A high-resolution TEM (HRTEM) image given in Figure 4b reveals further that the CdS NBs are structurally perfect. The measured spacing of the crystallographic planes is 0.33 nm, which corresponds to the {002} lattice plane of hexagonal CdS. The HRTEM image and SAED pattern reveal clearly that the CdS NBs are structurally uniform and single-crystalline. Moreover, there is a thin amorphous layer with a thickness of about 2 nm

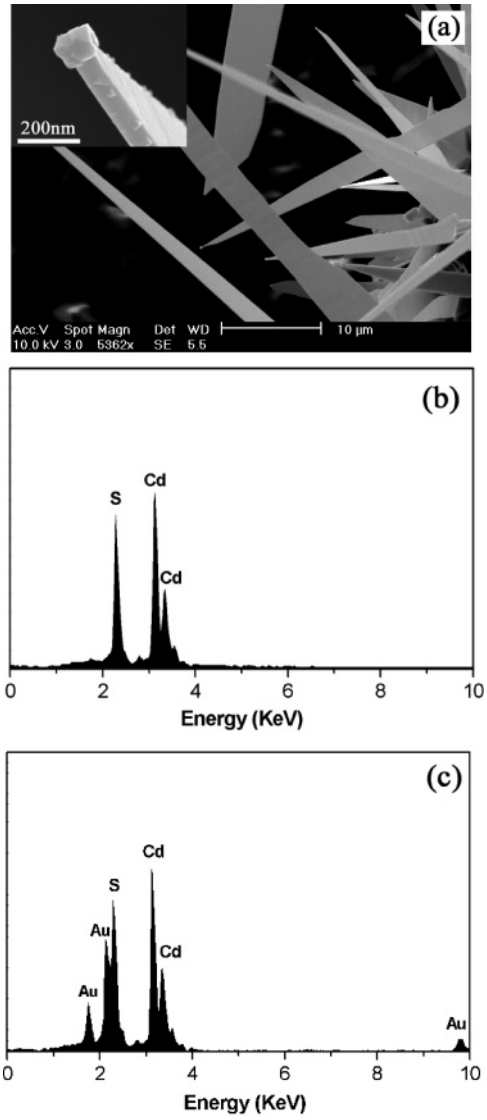

Figure 3. (a) FE-SEM image of the CdS NBs with variational widths and particle-like materials on their tips. The inset of (a) shows an individual belt capped by a particle. (b) and (c) are the corresponding EDS spectra taken from the CdS stem and the particle shown in the inset of (a).

that covers the surfaces (see Figure 4b), which would be the oxide formed during the TEM sample preparation.

3.2. Growth Mechanism of CdS NBs. Over the past few years, a variety of synthetic methods have been developed to produce a number of interesting NBs of materials from semiconductors[1,10−27] to metals.[37] Current research interest focuses on understanding the growth mechanism to obtain NBs of desired size and morphology, which are among the most important factors in determining their properties. The most conventional synthetic method for the NB system is VS growth.[1,7,12−20] Another approach for the vapor-phase growth of NBs is based on a catalyst-assisted VLS mechanism.[32] However, detailed processes leading to formation of beltlike 1D nanostructures with high width-to-thickness ratios are not well understood.

In the present case, we suggest that the CdS NBs would grow via a Au-catalyzed VLS process. This is consistent with previous reports[24,25,32] and is also supported by several experimental observations. For example, it is found that no CdS NBs could be obtained on the Si substrates by thermal evaporation of CdS powder at the same experimental conditions but in the absence

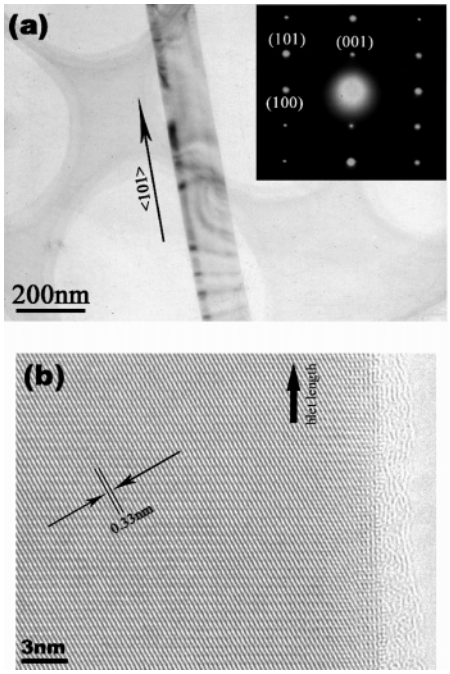

Figure 4. (a) TEM image of a CdS nanobelt. The inset shows its corresponding SAED pattern. (b) HRTEM image of the CdS nanobelt shown in (a).

of Au, indicating that the formation of the CdS NBs is initiated by Au catalyst particles. On the other hand, a characteristic of the VLS growth process is the existence of metal nanoparticles capped at the end of the produced nanostructures,[3,8] which is consistent with the observation of Au−CdS alloy at the tip of our CdS NBs shown in Figure 3. In the present experimental conditions, CdS vapor is rapidly generated at relatively high temperature by vaporizing the CdS powders. It is known that a thin Au film coated on the Si substrates would split into small Au liquid droplets at elevated temperatures.[36] These liquid Au droplets can serve as ideal nucleation sites for the preferential absorption of the evaporated CdS gas due to its large accommodation coefficient.[8,22] Continuous dissolution of Cd and S atoms in the Au−CdS eutectic alloy droplets will lead to the nucleation and growth of CdS NBs through the VLS process when the alloy droplets become saturated with reactant.[8,9] This Au-catalyzed VLS process is similar to that used previously for the growth of CdS NWs.[8,34]

However, due to the rectangular cross section and high width-to-thickness ratio of the CdS NBs, the above-mentioned VLS process is expected to be different from the conventional VLS process for the CdS NWs.[8,34] Generally, the factors that affect crystal growth kinetics may play important roles in determining the size and morphology of the final products, such as ambient gas,[38] pressure,[39] and temperature.[22,40] In the present work, it is found that CdS can grow into either NWs or NBs depending mainly on the growth temperature. Figure 5 shows the typical FE-SEM images taken from the as-synthesized CdS nanostructures on the Si substrates located in different positions corresponding to the different deposition temperatures. It can be seen that there are two kinds of CdS 1D nanostructures, NWs (Figure 5a) and NBs (Figure 5b). Figure 5c shows schematically the formation temperatures of these morphologies. The CdS NBs grow mainly in the temperature range 630−680 °C (region I in Figure 5c). In a temperature range of 580−630 °C (region II in Figure 5c), the produced CdS nanostructures are mainly NWs with Au catalyst particles capped at the wires' ends.[8,34] Moreover, it is found that the CdS NWs are grown along the

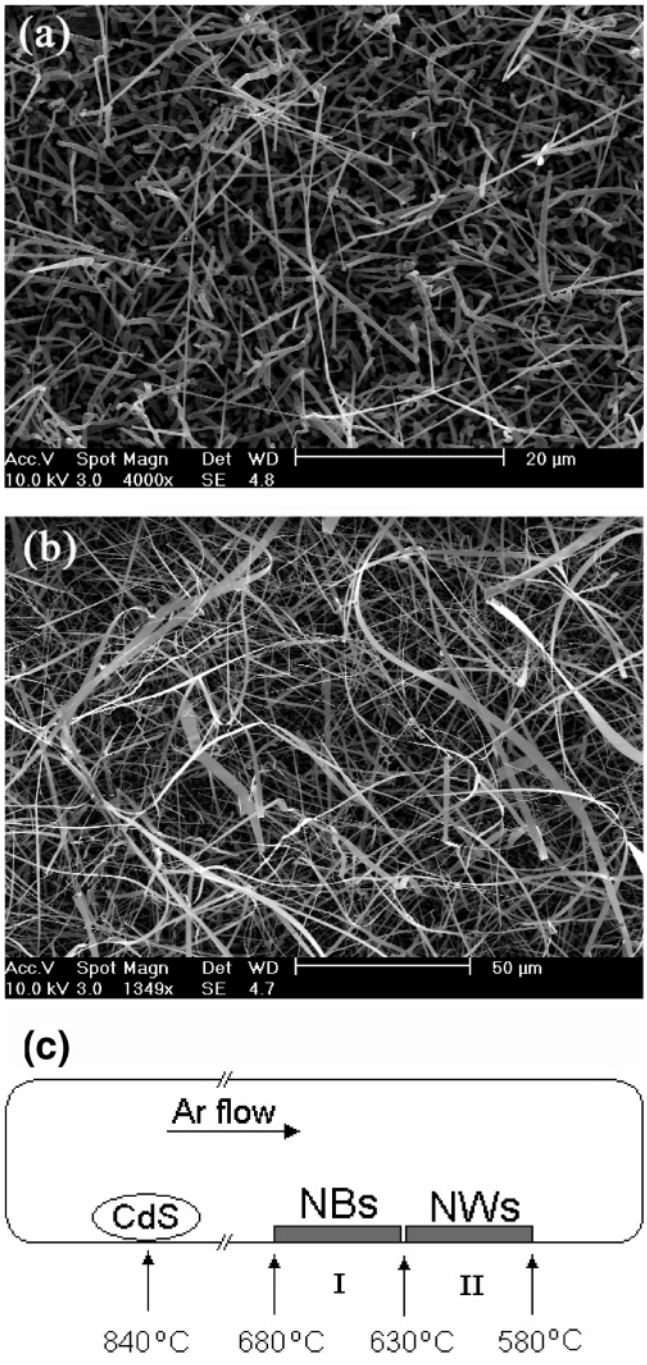

Figure 5. FE-SEM images showing the typical morphologies of the as-synthesized CdS nanostructures grown at different temperatures: (a) CdS NWs and (b) CdS NBs. (c) Schematic diagram showing the formation temperatures of these morphologies. The growth time is 1 h.

⟨101⟩ direction, which is similar to that of the CdS NBs. This reveals that both the CdS NBs and NWs are grown via the Au-catalyzed VLS mechanism along similar growth directions and a high growth temperature favors the formation of NBs. It has also been pointed out by several other researchers during their research of oxide NWs and NBs that the growth of NBs prefers higher temperature conditions.[1,10] However, the unambiguous role of growth temperature in the morphology of 1D nanostructures is unclear.[22,24]

We suspect that the dominant effect of the temperature is most likely on the growth rate along different crystal planes. This means that, during the Au-catalyzed VLS process, a higher temperature would favor the side growth along some favorable growth directions of a wurtzite-structured CdS crystal. Previously, Si needlelike and belt structures have been synthesized,[41] and some favorable growth directions have been suggested to be responsible for the belt structure growth.[42] Moreover, the side growth process due to the VS deposition has previously been discussed in the case of the NW system.[39] Obviously, the growth rate of the catalyst-assisted VLS process is much faster than that of the VS side growth,[39] which would be the possible reason for the formation of NB systems with a rectangular cross section and high width-to-thickness ratio. A schematic illustration of this proposed growth mode for the CdS NBs in this work is given in Figure 6. One may notice that the morphology of the CdS NBs is generally controlled by both the axial growth and the side growth. The above-mentioned growth mechanism of the CdS NBs is also consistent with the experimental observations. For example, the produced CdS NBs always possess a variational width along their length due to the side growth (see, for example, Figure 3a). This is also similar to a previous report of the ZnS NB growth by Hu et al.[24] However, the variational width of CdS NBs is mainly observed at the growth front of the belts,[24] the details of which are unclear at this stage.

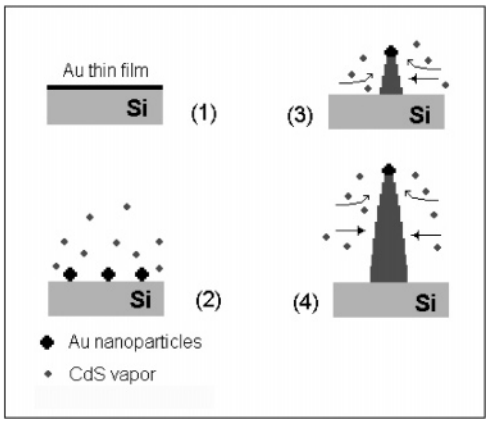

Figure 6. A schematic illustration of the vapor-phase growth of CdS NBs with the assistance of Au catalysts at high temperature. (1)−(4) show the different stages of the belt growth.

Since the growth of CdS nanobelts is initiated by Au catalyst nanoparticles via the catalyst-assisted VLS process, there is a possibility for the control of CdS NBs on such a special substrate as a Si wafer used in this work. First, it is found that the diameters of the Au catalyst particles are usually larger than the thickness of the produced belts (see the inset of Figure 3a), suggesting the thickness of the CdS NBs could be adjusted by using Au catalysts with suitable sizes. This phenomenon is somewhat similar to that of the Au-catalyzed VLS growth of semiconductor NWs reported previously.[36] Second, the side growth of CdS NBs via the VS process has little effect on the belt thickness (see, for example, Figure 3a); consequently, the increase of the CdS NB lengths and widths could be achieved by prolonging the growth time. This is thought to result from the catalyst-assisted VLS growth of CdS NBs along the belt length direction, which usually has a faster growth rate than that of the VS process along the width direction. The controlled synthesis of semiconductor NBs on a special substrate would be of great potential for their applications in both fundamental research and technological applications.

3.3. Luminescence Properties of CdS NBs. The optical properties of the CdS NBs have been investigated by PL to further assess their quality. The room-temperature PL spectrum of CdS NBs is shown in Figure 7. The CdS NBs feature two emission bands: one green band and another infrared one. Detailed analysis shows that the green emission of our CdS

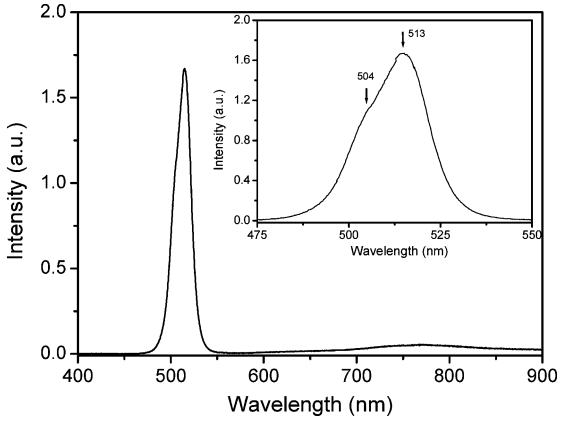

Figure 7. Room-temperature photoluminescence emission spectrum of the CdS NBs. The inset shows the details of the green emission band.

nanobelts has an intensive peak centered around 513 nm and a lower shoulder around 504 nm, as shown in the inset of Figure 7. The infrared emission band, from 700 to 850 nm and with a center around 770 nm, is broad and weak. Although the luminescence properties of CdS nanocrystals have been widely studied,[8,26,28−31,34,35] a few studies have been done on the luminescence properties of CdS NBs.[26] It is worthwhile to note that the overall features of our spectrum differ from those of previous ones.

We believe that the weak infrared luminescence band arises from transitions of electrons trapped at surface states to the valence band of CdS NBs. It is reasonable that there are surface and subsurface defects in the CdS NBs due to not only their large surface-to-volume ratio but also their chemical activity to react with oxygen when they are exposed to air.[22,23] The trap-state emissions related to surface defects of CdS have also been observed in the case of thin CdS films[43] and CdS NWs.[34] The energy of the 513 nm band agrees fairly well with the band gap of bulk CdS (2.42 eV at room temperature); therefore, it can be identified as the gap or band-to-band emission.[35] However, at present it is very difficult to unambiguously identify the origins of the 504 nm emission bands observed. Possibly, they can be attributed to a higher level transition or band-edge luminescence arising from the recombination of excitons and/or shallowly trapped electron−hole pairs. Experiments attempting to clarify the origins of the 504 nm emission band are currently under way, and results will be reported elsewhere.

4. Conclusions

We have successfully prepared CdS nanobelts in bulk quantities by thermally evaporating CdS powders under controlled conditions via a Au-catalyzed VLS process. The as-synthesized CdS nanobelts are single-crystalline with wurtzite structure, usually several tens of micrometers in length and several hundred nanometers in width. The thickness of the CdS nanobelts is in the range of 30−60 nm. The growth of CdS nanobelts is initiated by Au catalyst nanoparticles via a catalyst-assisted vapor−liquid−solid process. A side growth along the belt width direction via the VS process is also suggested in determining the morphology of the CdS NBs. The room-temperature PL spectrum of the as-synthesized CdS nanobelts has three luminescence bands around 504, 513, and 770 nm, which may be ascribed to band-edge, band-to-band, and surface state emissions, respectively.

Acknowledgment. This work is financially supported by the Special Funds for Major State Basic Research Project (Grant No. G2001CB3095) and the National Natural Science Foundation of China (Grant Nos. 69925410 and 60236010). T.G. thanks the China Postdoctoral Science Foundation for financial support.

References and Notes

(1) Pan, Z. W.; Dai, Z. R.; Wang, Z. L. *Science* **2001**, *291*, 1947.
(2) Iijima, S. *Nature* **199**1, *354*, 56.
(3) Hu, J.; Odom, T. W.; Liber, C. M. *Acc. Chem. Res*. **1999**, *32*, 435.
(4) Law, M.; Kind, H.; Messer, B.; Kim, F.; Yang, P. *Angew. Chem., Int. Ed.* **2002**, *41*, 2405.
(5) Comini, E.; Faglia, G.; Sberveglieri, G.; Pan, Z. W.; Wang, Z. L. *Appl. Phys. Lett*. **2002**, *81*, 1869.
(6) Hughes, W. L.; Wang, Z. L. *Appl. Phys. Lett*. **2003**, *82*, 2886.
(7) Arnold, M. S.; Avouris, P.; Pan, Z. W.; Wang, Z. L. *J. Phys. Chem. B* **2003**, *107*, 659.
(8) Barrelet, C. J.; Wu, Y.; Bell, D. C.; Lieber, C. M. *J. Am. Chem. Soc*. **2003**, *125*, 11498.
(9) Duan, X.; Lieber, C. M. *Adv. Mater*. **2000**, *12*, 298.
(10) Yao, B. D.; Chan, Y. F.; Wang, N. *Appl. Phys. Lett*. **2002**, *81*, 757.
(11) Li, Y. B.; Bando, Y.; Sato, T.; Kurashima, K. *Appl. Phys. Lett*. **2002**, *81*, 144.
(12) (a) Kong, X. Y.; Wang, Z. L. *Appl. Phys. Lett*. **2004**, *84*, 975. (b) Kong, X. Y.; Ding, Y.; Yang, R.; Wang, Z. L. *Science* **2004**, *303*, 1348.
(13) Dai, Z. R.; Pan, Z. W.; Wang, Z. L. *Solid State Commun*. **2001**, *118*, 351.
(14) Hu, J. Q.; Ma, X. L.; Shang, N. G.; Xie, Z. Y.; Wong, N. B.; Lee, C. S.; Lee, S. T. *J. Phys. Chem. B* **2002**, *106*, 3823.
(15) (a) Sun, S. H.; Meng, G. W.; Zhang, G. X.; Gao, T.; Geng, B. Y.; Zhang, L. D.; Zuo, J. *Chem. Phys. Lett*. **2003**, *376*, 103. (b) Zhang, J.; Jiang, F.; Zhang, L. *J. Phys. D: Appl. Phys*. **2003**, *36*, L21.
(16) Dai, Z. R.; Pan, Z. W.; Wang, Z. L. *J. Phys. Chem. B* **2002**, *106*, 902.
(17) Zhang, J.; Zhang, L. *Solid State Commun*. **2002**, *122*, 493.
(18) (a) Ma, R.; Bando, Y. *Chem. Phys. Lett*. **2003**, *370*, 770. (b) Li, Y.; Bando, Y.; Sato, T. *Chem. Phys. Lett*. **2002**, *359*, 141.
(19) Zhang, J.; Zhang, L. *Chem. Phys. Lett*. **2002**, *363*, 293.
(20) Ma, C.; Moore, D.; Li, J.; Wang, Z. L. *Adv. Mater*. **2003**, *15*, 228.
(21) Jang, Y.; Meng, X. M.; Liu, J.; Xie, Z. Y.; Lee, C. S.; Lee, S. T. *Adv. Mater*. **2003**, *15*, 323.
(22) Li, Q.; Wang, C. *Appl. Phys. Lett*. **2003**, *83*, 359.
(23) Zhu, Y. C.; Bando, Y.; Xue, D. F. *Appl. Phys. Lett*. **2003**, *82*, 1769.
(24) Hu, P.; Liu, Y.; Fu, L.; Cao, L.; Zhu, D. *J. Phys. Chem. B* **2004**, *108*, 936.
(25) Dong, L.; Jiao, J.; Coulter, M.; Love, L. *Chem. Phys. Lett*. **2003**, *376*, 653.
(26) Ip, K. M.; Wang, C. R.; Li, Q.; Hark, S. K. *Appl. Phys. Lett*. **2004**, *84*, 795.
(27) Zhang, J.; Jiang, F.; Zhang, L. *J. Phys. Chem. B* **2004**, *108*, 7002.
(28) Agata, M.; Kurase, H.; Hayashi, S.; Yamamoto, K. *Solid State Commun*. **1990**, *76*, 1061.
(29) Ullrich, B.; Bagnall, D. M.; Sakai, H.; Segawa, Y. *Solid State Commun*. **1999**, *109*, 757.
(30) Artemyev, M. V.; Sperling, V.; Woggon, U. *J. Appl. Phys*. **1997**, *81*, 6975.
(31) Duan, X. F.; Huang, Y.; Agarwal, R.; Lieber, C. M. *Nature* **2003**, *421*, 241.
(32) Wang, Z.; Pan, Z. *Adv. Mater*. **2002**, *14*, 1029.
(33) Wagner, R. S.; Ellis, W. C. *Appl. Phys. Lett*. **1964**, *4*, 89.
(34) Wang, Y.; Meng, G.; Zhang, L.; Liang, C.; Zhang, J. *Chem. Mater*. **2002**, *14*, 1773.
(35) Gudiksen, M. S.; Lieber, C. M. *J. Am. Chem. Soc*. **2000**, *122*, 8801.
(36) Huang, M. H.; Wu, Y. Y.; Feick, H.; Tran, N.; Weber, E.; Yang, P. D. *Adv. Mater*. **2001**, *13*, 113.
(37) Wang, Y.; Zhang, L.; Meng, G.; Liang, C.; Wang, G.; Sun, S. *Chem. Commun*. **2001**, 2632.
(38) Zhang, Y. F.; Tang, Y. H.; Peng, H. Y.; Wang, N.; Lee, C. S.; Bello, I.; Lee, S. T. *Appl. Phys. Lett*. **1999**, *75*, 1842.
(39) (a) Chen, X. L.; Lan, Y. C.; Li, J. Y.; Cao, Y. G.; He, M. *J. Cryst. Growth* **2001**, *222*, 586. (b) Chen, X. L.; Li, J. Y.; Lan, Y. C.; Cao, Y. G. *Mod. Phys. Lett. B* **2001**, *15*, 27.
(40) Wang, X. D.; Gao, P. X.; Li, J.; Summers, C. J.; Wang, Z. L. *Adv. Mater*. **2002**, *14*, 1732.
(41) Greiner, E. S.; Gutowski, J. A.; Ellis, W. C. *J. Appl. Phys*. **1961**, *32*, 2489.
(42) Wagner, R. S.; Treuting, R. C. *J. Appl. Phys*. **1961**, *32*, 2490.
(43) (a) Bouchenaki, C.; Ullrich, B.; Zielinger, J. P. *J. Lumin*. **1991**, *48/49*, 649. (b) Feldman, B. J.; Duisman, J. A. *Appl. Phys. Lett*. **1981**, *37*, 1092.